atmosphere

MDPI

Article

Chemical Fractionation of Trace Elements in Arctic PM_{10} Samples

Eleonora Conca [1], Mery Malandrino [1,*], Agnese Giacomino [2], Paolo Inaudi [2], Annapaola Giordano [3], Francisco Ardini [4], Rita Traversi [5] and Ornella Abollino [2]

1 Department of Chemistry, University of Turin, 10125 Torino, Italy; eleonora.conca@unito.it
2 Department of Drug Science and Technology, University of Turin, 10125 Torino, Italy; agnese.giacomino@unito.it (A.G.); paolo.inaudi@unito.it (P.I.); ornella.abollino@unito.it (O.A.)
3 Department of Agricultural, Forest and Food Sciences, University of Turin, 10125 Torino, Italy; annapaola.giordano@unito.it
4 Department of Chemistry and Industrial Chemistry, University of Genoa, 16146 Genova, Italy; ardini@chimica.unige.it
5 Department of Chemistry "Ugo Schiff", University of Florence, 50019 Sesto Fiorentino, Italy; rita.traversi@unifi.it
* Correspondence: mery.malandrino@unito.it; Tel.: +39-0116705249

Abstract: In this study, the information potential of a two-step sequential extraction procedure was evaluated. For this purpose, first of all the elemental composition of Arctic PM_{10} samples collected in Ny-Ålesund (Svalbard Islands) from 28 February 2015 to 21 October 2015 was investigated. Enrichment Factors, Principal Component Analysis and Hierarchical Cluster Analysis were performed to identify PM_{10} sources and to understand the effects of short- and long-range transport processes. The investigation of the potential source areas was also aided by taking into account back-trajectories. Then, the sequential extraction procedure was applied to some of the samples in order to obtain more information on these sources. This approach allowed us to establish that most of the elements prevalently having an anthropogenic origin not only were present in higher concentrations, but they were also more easily extractable in late winter and early spring. This confirms the common statement that the anthropogenic portion of the elements present in a sample is generally loosely bound to the particulate matter structure, and so it is more easily extractable and releasable on the Arctic snowpack. Moreover, in the samples collected in late winter and early spring, even the elements prevalently having a crustal origin were more easily extractable, probably due to the particle size selection occurred during the long-range transport.

Keywords: PM_{10}; Ny-Ålesund (Svalbard Islands); trace elements; sequential extraction; source identification; Arctic haze

Citation: Conca, E.; Malandrino, M.; Giacomino, A.; Inaudi, P.; Giordano, A.; Ardini, F.; Traversi, R.; Abollino, O. Chemical Fractionation of Trace Elements in Arctic PM_{10} Samples. *Atmosphere* **2021**, *12*, 1152. https://doi.org/10.3390/atmos12091152

Academic Editor: Andrés Alastuey Urós

Received: 7 July 2021
Accepted: 3 September 2021
Published: 7 September 2021

1. Introduction

It is widely recognised that the global climate change is first perceptible in the polar regions, due to alterations of water mass distribution and sea ice extension. It is known that the Arctic warming is occurring much more rapidly than the global average, and in particular, the Ny-Ålesund archipelago has experienced a significant rise in temperature over the last two decades [1,2]. Moreover, polar areas play a key role in regulating biogeochemical cycles, and hence the global climatic system, through complex "feedback" mechanisms. The understanding of the mechanisms regulating the interaction among air, oceans and ice in these areas is essential to predict the effects of the changes observed in the climate. In this scenario, the study of the chemical composition of atmospheric particulate matter in Arctic, the understanding of the transport mechanisms by which inorganic pollutants emitted in temperate and tropical areas reach Arctic and the possibility to interrelate this information with complementary features are important to understand the effect exerted by

the climatic conditions on this area, as well as to highlight possible tendencies or anomalies of behaviour and future evolutions [3–6].

With this aim, it is important to know both total concentration and reactivity and availability of the metal species. In fact, although solubility depends on the chemical nature of compounds and particles considered, the distinction between soluble and insoluble fractions in the Arctic atmospheric aerosol may have two main applications: the identification of the relative contributions of different natural and anthropogenic sources of aerosol (for example continental, biogenic and marine); the understanding, on one hand, of the processes of generation and transport at short and long distance of the aerosol in Arctic and, conversely, of the tendency of the metals associated with atmospheric particulate solid phases to enter into biogeochemical cycles.

The determination of trace elements in airborne particulate matter samples (PM) collected in polar environments is generally performed by means of a direct microwave-assisted acid digestion [7–9]. Even though the determination of such low concentrations certainly requires the adoption of precautions to avoid contamination, this procedure is relatively easy and allows an accurate determination of PM element composition. However, in this way, it is not possible to distinguish the different chemical forms in which the elements are present in the samples.

The procedures allowing this distinction are called "speciation" and can be a useful tool for source apportionment studies, i.e., for studies focused on the source and provenance identification of the PM. Nevertheless, in practice, proper speciation is not easy to perform, and it is generally substituted by fractionation through sequential extraction procedures [10–14]. The latter have an operational nature and simply provide a classification of analytes according to their chemical properties (i.e., solubility) [12,15]. However, it is generally recognised that the anthropogenic portion of the elements in PM is more easily extractable than the crustal one [16,17].

Different extracting solutions, extraction methods, and techniques for the separation of the extract from the solid residue are currently used for the fractionation purpose, thus reducing the possibility to compare results obtained in different studies [11,13,18–20]. In a previous study, the most common extracting solutions (namely high purity water (HPW), 0.032 M HNO_3, 0.022 M HCl, 0.11 M CH_3COOH, and 0.012 M CH_3COOH/CH_3COONH_4 buffer) and extraction methods (namely 16 h stirring and 15 min ultrasounds) used for the first step of element fractionation in PM were compared, in order to identify the procedure which gives the best estimation of the anthropogenic portion of the elements present in Arctic PM_{10} samples [21].

In this study, the information potential of the optimized two-step sequential extraction procedure (i.e., 0.032 M HNO_3 and 16 h stirring, followed by a microwave-assisted acid digestion) was evaluated considering selected Arctic PM_{10} samples collected in Ny-Ålesund (Svalbard Islands, Norwegian Arctic) in 2015. Firstly, the elemental composition was determined by microwave digestion. Then, the sequential extraction procedure was applied to selected samples, in order to evaluate the different mobility and reactivity of the elements, which in turn determine their behaviour at the air-snow and air-ocean interfaces, and obtain more information on the PM_{10} sources. A wide variety of elements was determined, i.e., Al, As, Ba, Ca, Cd, Co, Cr, Cu, Fe, K, Mg, Mn, Na, Ni, Pb, Sb, Ti, V and Zn. To the best of our knowledge, our study is the first in which a fractionation procedure was applied to a large number of Arctic PM_{10} samples, although fractionation studies have already been performed in polar areas, namely on the Antarctic atmospheric particulate matter [10,13,14].

2. Materials and Methods

2.1. Study Area and Sampling

Ny-Ålesund (78°55′30″ N, 11°55′40″ E) is a small Arctic settlement mainly devoted to scientific research and environmental monitoring. It is located in the Norwegian Svalbard archipelago and, more precisely, in the Kongsfjorden, on the western coast of Spitsbergen Island [8]. The aerosol sampling was performed at the Gruvebadet atmospheric laboratory

(40 m a.s.l.), situated about 800 m far from Ny-Ålesund. The location was established in order to minimize the influence of local pollution during measurements, which is kept low thanks to the prevailing wind direction (115° N) [22]. Moreover, a meteo-trigger system was used during sampling, in order to switch off the sampling devices when the wind was absent (<0.5 m/s) or came from the town [8,9].

A total of 58 PM_{10} samples were collected with a 4-days resolution during the 2015 sampling campaign, which started on 28 February and ended on 21 October. For the sake of brevity, the samples are named throughout the manuscript according to the sampling start date. The sampling took place by means of PTFE hydrophilic filters (Advantec, product code: H100A090C, 90 mm diameter, efficiency >99% for 0.3 µm particles) and an Echo HiVol sampler (TCR Tecora, 200 L/min). These filters have been used in previous studies [7,8,21] and featured extremely reproducible and low blanks. Before shipping them to the Gruvebadet station for the present sampling campaign, several filters were tested in laboratory to ensure their good performance with regard to blank values. Moreover, it should be noted that all the filters used in the 2015 sampling campaign derive from the same batch. The collected samples were placed in polycarbonate Petri dishes, sealed and immediately frozen at −20 °C; this temperature was maintained during all stages of transportation to Italy and storage.

2.2. Apparatus and Reagents

A Milestone ETHOS One microwave laboratory unit was used for both the direct digestion of PM_{10} samples and for the dissolution of the solid residues. According to the concentration levels, the analyses of extracts and mineralized residuals were carried out using a sector-field inductively coupled plasma mass spectrometer (SF-ICP-MS) or an inductively coupled plasma optical emission spectrometer (ICP-OES), as reported in the previous work [21]. For all the elements analysed in PM_{10} samples and in the samples obtained by applying the sequential extraction (Fraction I and II), the adopted operating conditions, experimentally determined limits of detection (LOD) and sample blanks (SB) are reported in Supplementary Tables S1 and S2, respectively. LOD values represent the analyte concentration corresponding to three times the standard deviation of the reagent blank. Sample blanks were prepared similarly to the samples, both by directly digesting and applying the sequential extraction procedure to some blank filters which had undergone the transport to and from the sampling site; SB concentrations were subtracted from sample concentrations, in order to eliminate the filter, travel, and storage contributions.

The nitric acid used both for the preparation of the extracting solution and for the microwave digestion was further purified by sub-boiling (s.b.) distillation in a quartz apparatus, from a 65% analytical grade solution. For the digestion of samples, ultrapure (u.p.) hydrogen peroxide (30%) was also used. Water was purified in a Milli-Q system, resulting in high purity water (HPW) with a resistivity of 18 MΩ·cm. Appropriate standard solutions were prepared from concentrated (1000 mg L^{-1}) single element solutions (Merck Millipore, Darmstadt, Germany).

2.3. Direct Digestion of PM_{10} Samples

For the direct digestion of samples, one quarter of each filter was used. The microwave-assisted digestion was performed in 30 mL tetrafluoromethoxyl vessels, which were then inserted into 100 mL tetrafluoromethoxyl vessels, according to the so-called "vessel-inside-vessel technology" [23]. The digestion mixture was composed of 2 mL s.b. HNO_3 and 0.5 mL u.p. H_2O_2, according to the standard method for the measurement of Pb, Cd, As and Ni in the PM_{10} fraction of suspended particulate matter (UNI EN 14902:2005), while a mixture of 10 mL HPW and 1 mL analytical grade H_2O_2 was introduced in the bigger vessel. The temperature was ramped to 220 °C within 20 min and then kept constant at 220 °C for 20 min. After the digestion, the obtained solution was filtered through a Whatman Grade 5 cellulose filter (porosity 2.5 µm) to remove any insoluble particles and HPW was added up to 15 mL. Prior to digestion, the samples were left in contact with the

digestion mixture for approximately 16 h, in order to ensure the complete impregnation of the filter.

All the steps of the analytical procedure (e.g., filter cuts and digestion preparation) were performed, whenever possible, under a Class-100 laminar flow hood. The reagent blanks, used for preparing the calibration standard solutions, were obtained by microwave-digesting the reagent mixture only. Calibration checks were run at frequent intervals (three times for each hour) during the analysis sequence.

2.4. Sequential Extraction of PM_{10} Samples

For the sequential extraction, 24 samples were selected. In this case, one half of each filter was used, and the procedure optimized in [20], and briefly described hereafter, was applied. The filter was cut into small pieces and immediately introduced into a 30 mL polycarbonate bottle, together with 10 mL of 0.032 M s.b. HNO_3. The extraction was performed by stirring for 16 h at approximately 200 rpm. After the extraction, the suspension containing the insoluble fraction of the sample and the PTFE filter was vacuum-filtered through Advantec mixed cellulose ester filters. The solution (fraction I) was then acidified with 100 µL s.b. HNO_3, and HPW was added up to 20 mL. The membrane filter, containing the insoluble fraction of the sample, was subsequently cut into four pieces with stainless steel scissors and microwave-digested using the vessel-inside-vessel technology [23] for obtaining fraction II. The digestion mixture was composed of 2 mL s.b. HNO_3 and 0.5 mL u.p. H_2O_2, while a mixture of 10 mL HPW and 1 mL analytical grade H_2O_2 was introduced into the bigger vessel. The temperature was ramped to 220 °C within 20 min, followed by a dwell time of another 20 min. The obtained solution (fraction II) was subsequently filtered and HPW was added up to 20 mL. The extraction percentages were calculated with respect to the sum of fraction I and fraction II.

All the possible steps of the sequential extraction procedure were performed in a clean environment under a Class-100 laminar flow bench-hood, to avoid any possible contamination.

2.5. Data Analysis

For the graphical representation of the seasonal concentration trends, normalized values were used in order to eliminate the differences in concentration levels between elements. For this aim, all the concentration values were divided by the concentration of the first sample of the campaign [24]. In this way, the normalized value for each element in the first sample of the campaign (28 February) was always equal to 1.

Crustal and marine enrichment factors (CEFs and MEFs, respectively) were calculated as explained in [8], using Al and Na as reference elements [25,26]. The upper crust concentration reported by Wedepohl [27] and the average sea composition reported by Goldberg [28] were used for the purpose.

The datasets obtained by direct digestion and by sequential extraction of the PM_{10} samples were autoscaled and processed by Hierarchical Cluster Analysis (HCA) and Principal Component Analysis (PCA) using XlStat 2017 software package, an add-on of Microsoft Excel. Information on the principles of this technique can be found elsewhere [29–31].

2.6. HYSPLIT Back-Trajectories

Air mass back-trajectories were calculated using the NOAA HYSPLIT 4 transport model [32,33] and the GDAS meteorological data supplied by ARL (Air Resources Laboratory, College Park, MD, USA, http://ready.arl.noaa.gov, accessed on 22 July 2021). The back-trajectory starting point was the Gruvebadet laboratory (78.92° N, 11.89° E, 0.0 m AGL); the propagation time was 120 h and a new back-trajectory started every 6 h.

3. Results and Discussion

3.1. Direct Digestion of PM_{10} Samples

Table 1 reports the descriptive statistics of the element concentrations obtained from the direct digestion of all PM_{10} samples collected in 2015 while element concentrations (mean and standard deviation) in each PM_{10} sample are shown in Supplementary Tables S3 and S4; for converting the LOD from μg/L (or ng/L) to pg/m^3 (or fg/m^3), the actual solution volume and air volume of each sample were used and median and percentiles were calculated considering values below the LOD as equal to it.

Table 1. Descriptive statistics of the element concentrations obtained from the direct digestion of all PM_{10} samples collected in 2015. All the values are expressed in pg/m^3 except Al, Ca, Fe, K, Mg and Na, which are expressed in ng/m^3.

Statistics	Al	As	Ba	Ca	Cd	Co	Cr	Cu	Fe	K	Mg	Mn	Na	Ni	Pb	Sb	Ti	V	Zn
5th percentile	0.84	2.9	14	5.3	0.34	0.51	5.0	2.8	0.77	2.5	4.8	26	32	12	4.5	1.3	27	1.7	26
Median	3.9	8.4	51	14	0.95	2.0	33	23	2.8	6.0	18	100	130	27	23	3.4	196	13	72
95th percentile	22	77	210	42	13	9.9	130	150	17	28	90	540	650	110	360	25	850	47	830

As expected for Arctic PM_{10} samples, the concentrations were quite low, except for Al, Ca, Fe, K, Mg and Na, which generally have a natural origin. However, as it can be seen from the 5th and 95th percentiles, the concentrations exhibit a large variability throughout the sampling campaign. The elements having the lowest concentrations were Cd, Co and Sb. Cd showed a few concentration values below the LOD, precisely equal to 21% of the total, in the summer and early autumn. The other elements with concentrations below the LOD were Ti (for two samples) and Co, K and Zn (for one sample). The PM_{10} concentrations found in this campaign were comparable with the values determined during the previous Arctic spring-summer sampling campaigns carried out at Gruvebadet research station [8,9].

For trying to obtain a first subdivision of elements according to their sources, CEFs and MEFs were used. In this way, it was possible to identify elements prevalently having crustal (CEF < 10, MEF > 10), marine (MEF < 10, CEF > 10) or anthropogenic (CEF > 10, MEF > 10) origin [26,34,35]. The box plots of calculated CEFs and MEFs for all PM_{10} samples collected in 2015 are shown in Figure 1. From the graphs, it is possible to see that Ba, Co, Fe, Mn, Ti and V prevalently have a crustal origin, while Ca, K and Mg prevalently have a marine origin. Consequently, it is possible to infer an anthropogenic origin for all the other elements, i.e., As, Cd, Cr, Cu, Ni, Pb, Sb and Zn. However, it should be noted that some analytes prevalently deriving from crustal sources might also have, in some specific samples, an anthropogenic origin. This is evidenced in Figure 1a by the outliers of the box plots, which are sometimes quite higher than most of the other values.

For gaining better insights into the sources of the analysed elements, HCA was performed taking into account the results of the direct digestion of all PM_{10} samples collected in 2015. The dendrogram in Figure 2 reveals the presence of four main clusters. Two of them can be attributed to natural sources (i.e., Ca, K, Mg and Na to a marine source and Al, Ba, Co, Fe, Mn, Ti and V to a crustal source), and perfectly meet the results obtained from the enrichment factor calculation. Furthermore, the analytes prevalently having a non-natural origin form two distinct clusters: one composed by Cr and Ni only, and one composed by As, Cd, Pb, Sb, Zn and, at a higher level of dissimilarity, Cu. Therefore, it is possible to hypothesize two distinct sources for these two groups of elements. The latter cluster is mainly composed of analytes generally attributed to mid-latitude anthropogenic sources, hence deriving from long-range transport processes from North America or Russia [8,36]. Conversely, Cr and Ni can be attributed to air masses coming from southwest Greenland, an area where early rock minerals are particularly rich in these elements [5,37]. In fact, at a higher level of dissimilarity, Cr and Ni belong to the same cluster of the elements prevalently having a crustal origin, and this might confirm this hypothesis.

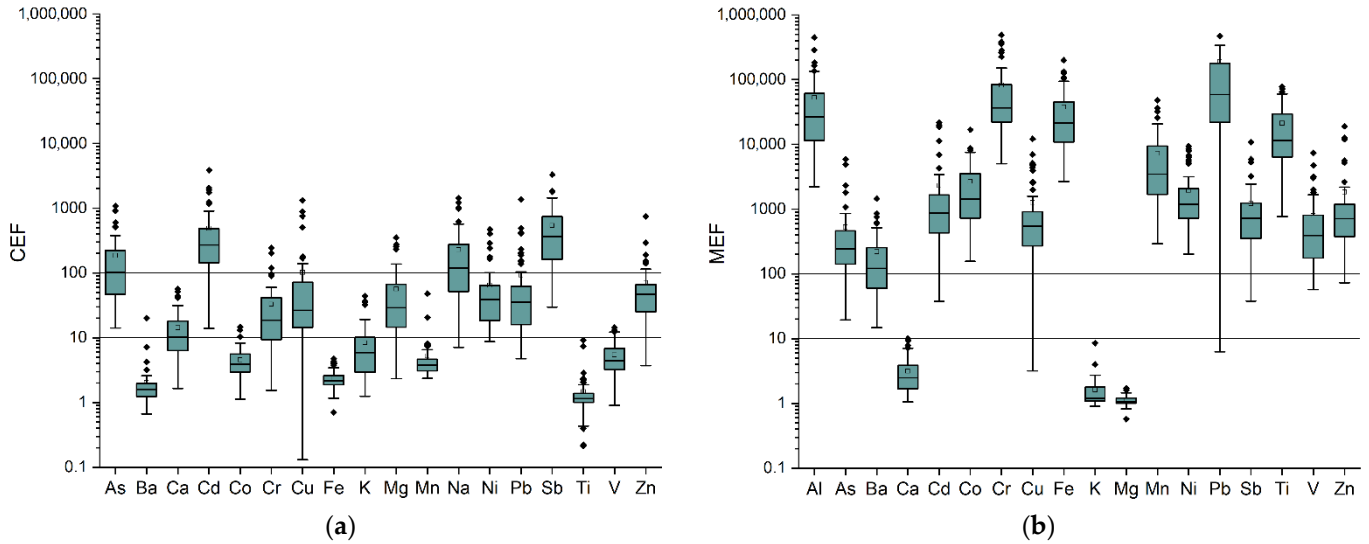

Figure 1. Box plots showing (**a**) crustal and (**b**) marine enrichment factors calculated for all PM_{10} samples collected in 2015.

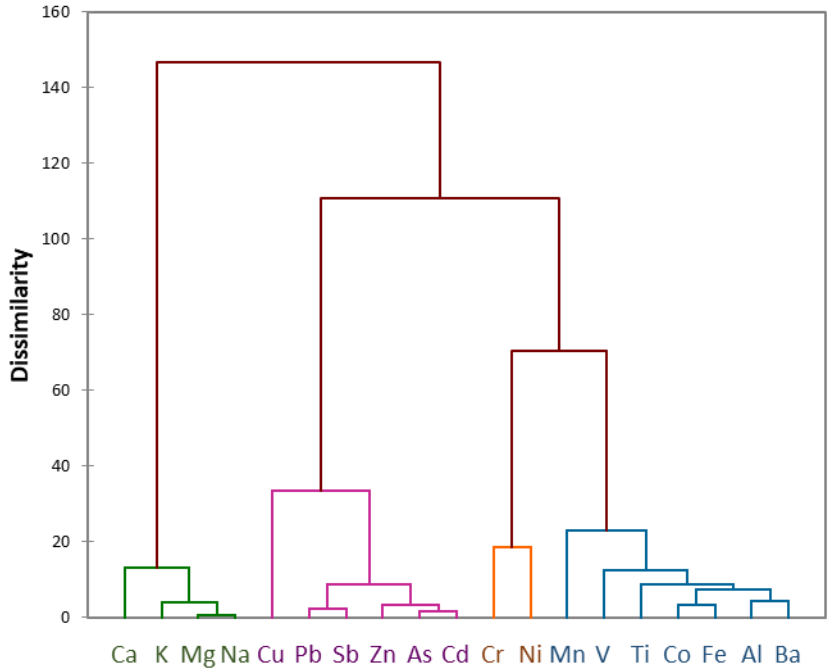

Figure 2. Dendrogram obtained by HCA on the results of the direct digestion of all PM_{10} samples collected in 2015.

Figure 3a–d shows the seasonal trends registered for the four clusters of elements emerged from HCA. In all cases, a strong correlation can be seen, as expected, for elements having a common origin. Two marked concentration peaks were registered in March and April for prevalently anthropogenic elements, thus confirming their probable mid-latitude origin (Figure 3a). Indeed, the phenomenon known as "Arctic haze", involving the long-range transport of air masses from mid-latitudes to the Arctic, is recognised to be particularly strong in winter and early spring [38–40]. As expected, the HYSPLIT back-trajectories calculated for the two spring samples (Figure 4a,b) having high concentrations, show that the air masses travelled long-distances before reaching Svalbard. In the first case, the air masses mainly came from Russia and North America (Greenland and Canada), but they also shortly travelled on a small part of Northern Europe lands. In the second

case, a marked contribution from Russia is evident, but some back-trajectories still came from Greenland.

The marked peaks registered for anthropogenic elements are also present in Figure 3b–d, indicating that the air masses deriving from mid-latitudes, passing over great areas of land and ocean, become also enriched of both crustal and marine elements. However, the concentrations of crustal elements in Figure 3b display some more peaks in late spring and summer, which generally coincide with the ones in Figure 3c. Therefore, it is possible to hypothesize that the trends registered for crustal elements are the result of two different sources, i.e., Arctic haze long-range transport (in early spring) and erosion of enriched soils of southwest Greenland. This hypothesis is coherent with the calculated HYSPLIT back-trajectories, even though, in Figure 4b, a propagation time of 5 days is not sufficient for verifying if the air masses travelled over Greenland. However, the propagation time of the HYSPLIT back-trajectories cannot exceed 5 days, since after that period, the uncertainty of the model becomes too high. Finally, the concentrations of marine elements (Figure 3d) and partially those of crustal elements (Figure 3b) and of Cr and Ni (Figure 3c) show higher values in the samples collected in September-early October: this trend indicates again a greater contribution of aerosol coming from Greenland, confirmed by the calculated HYSPLIT back-trajectories for 16 September sample (Figure 4c), but also of local sources (marine spray and resuspension of the local soil), to the composition of PM_{10} in this period (Figure 4d). This behaviour could depend on a greater ice-free sea and ground surface, which determines a greater contribution of local sources to the Arctic atmospheric aerosol.

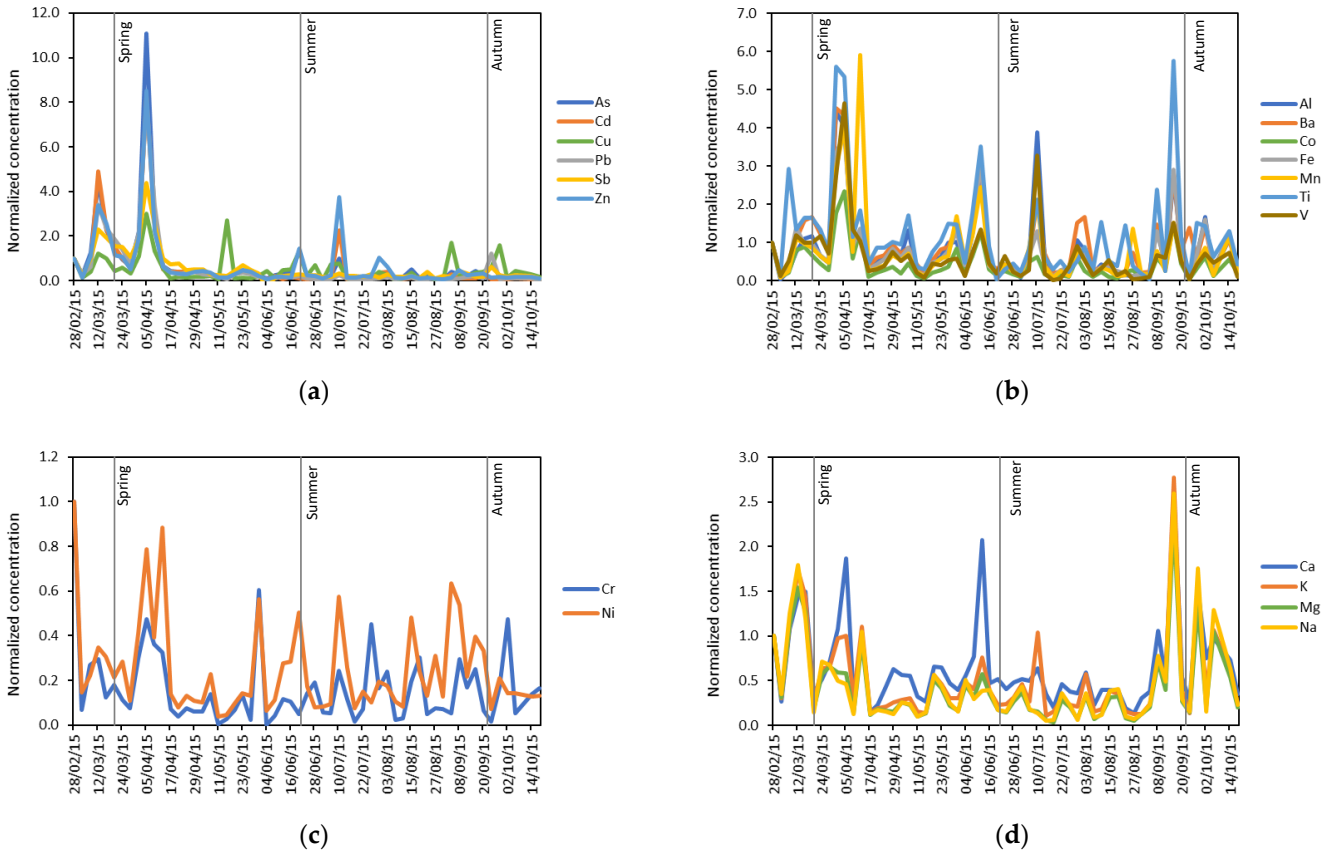

Figure 3. Seasonal trends registered for the four clusters of elements emerged from HCA: (**a**) As, Cd, Cu, Pb, Sb, Zn; (**b**) Al, Ba, Co, Fe, Mn, Ti, V; (**c**) Cr, Ni; (**d**) Ca, K, Mg, Na.

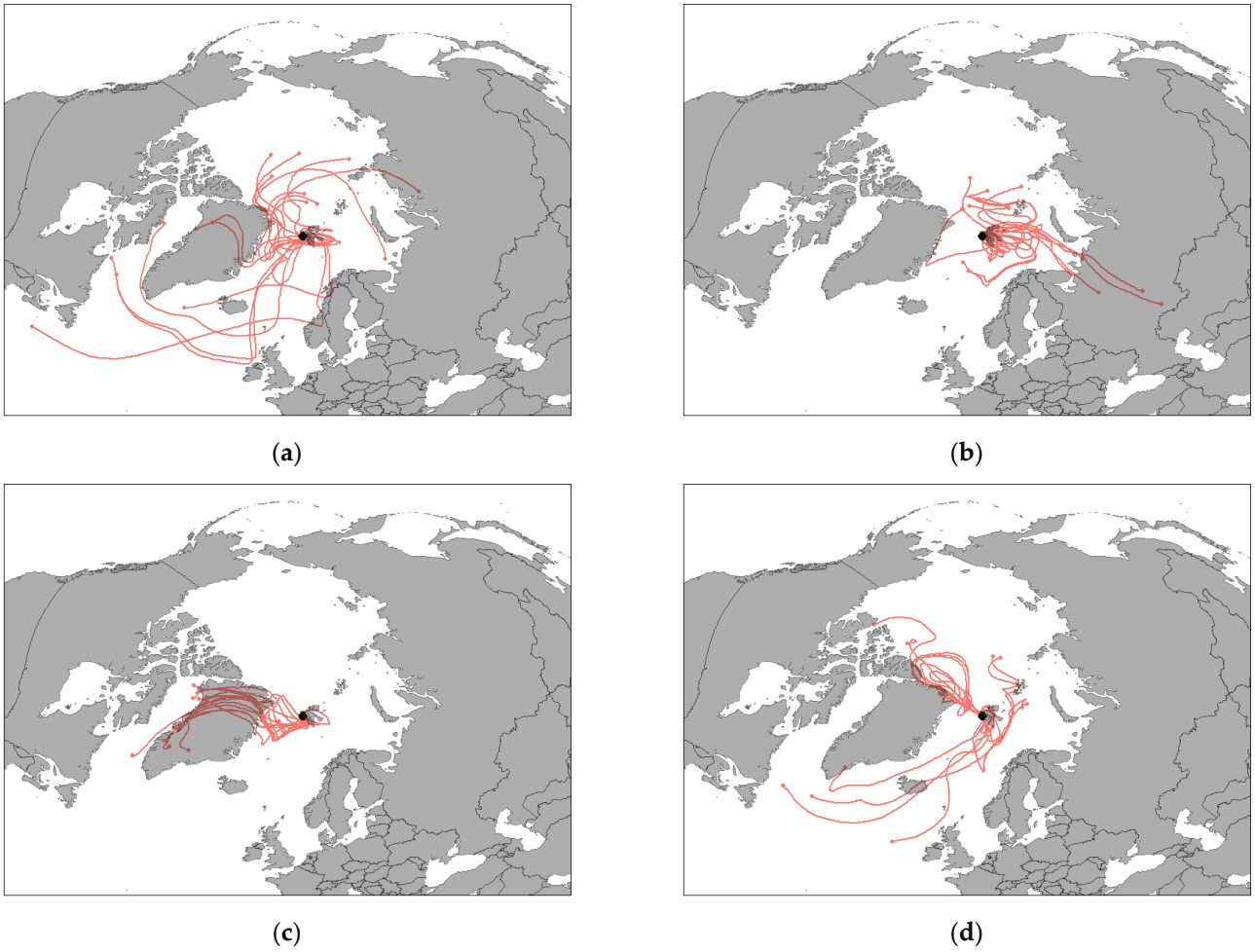

Figure 4. HYSPLIT back-trajectories calculated for two samples collected in spring: (**a**) 12 March, (**b**) 5 April; and for two samples collected in autumn: (**c**) 16 September and (**d**) 28 September.

3.2. Sequential Extraction of PM_{10} Samples

The results of the sequential extractions, expressed in percentages, are reported in Supplementary Table S5 and shown in Figure 5. The outcomes are generally coherent with the prevalent source of each analyte identified by means of CEFs and MEFs. Indeed, prevalently marine analytes (namely Ca, K, Mg and Na), which are generally present in the airborne particles in the form of soluble salts, were mostly present in fraction I (Figure 5a–d). Similarly, the analytes prevalently having an anthropogenic origin (namely As, Cd, Cu, Pb, Sb and Zn), which are generally weakly bound to the particles, were mainly extracted in fraction I (Figure 5e–j). Conversely, prevalently crustal analytes (namely Al, Ba, Co, Fe, Mn, Ti and V), which are generally strongly bound to the mineral structure of the particles, were mostly present in fraction II (Figure 5k–q). With regard to Cr and Ni, the hypothesis made in Paragraph 3.1 seems to be confirmed: regardless their high CEFs and MEFs, these analytes were not easily extractable, as expected for elements mainly having a crustal origin (Figure 5r,s). Moreover, it is noteworthy to observe that when the concentration of both crustal and marine and anthropogenic elements increases, their more labile fraction (fraction I) increases to a greater extent than the residual one (fraction II). This is evident, for example, for the 28 September sample in which the concentrations of crustal and marine elements increase and their percentage extracted in fraction I also increases. This insight is very useful to better understand the transport, deposition and bioaccumulation processes of some elements, such as Fe, Mn, Ni, Pb and Zn. Indeed, it is essential to know their solubility, reactivity, and availability in the atmospheric aerosol to

evaluate their behaviour at air/ocean/ice interfaces and the application of this two-step fractionation procedure, specifically developed and optimized for Arctic PM_{10}, permitted to distinguish among different forms of some important elements (e.g., Fe, Mn, Cu, etc.) having different solubility, reactivity, and releasability.

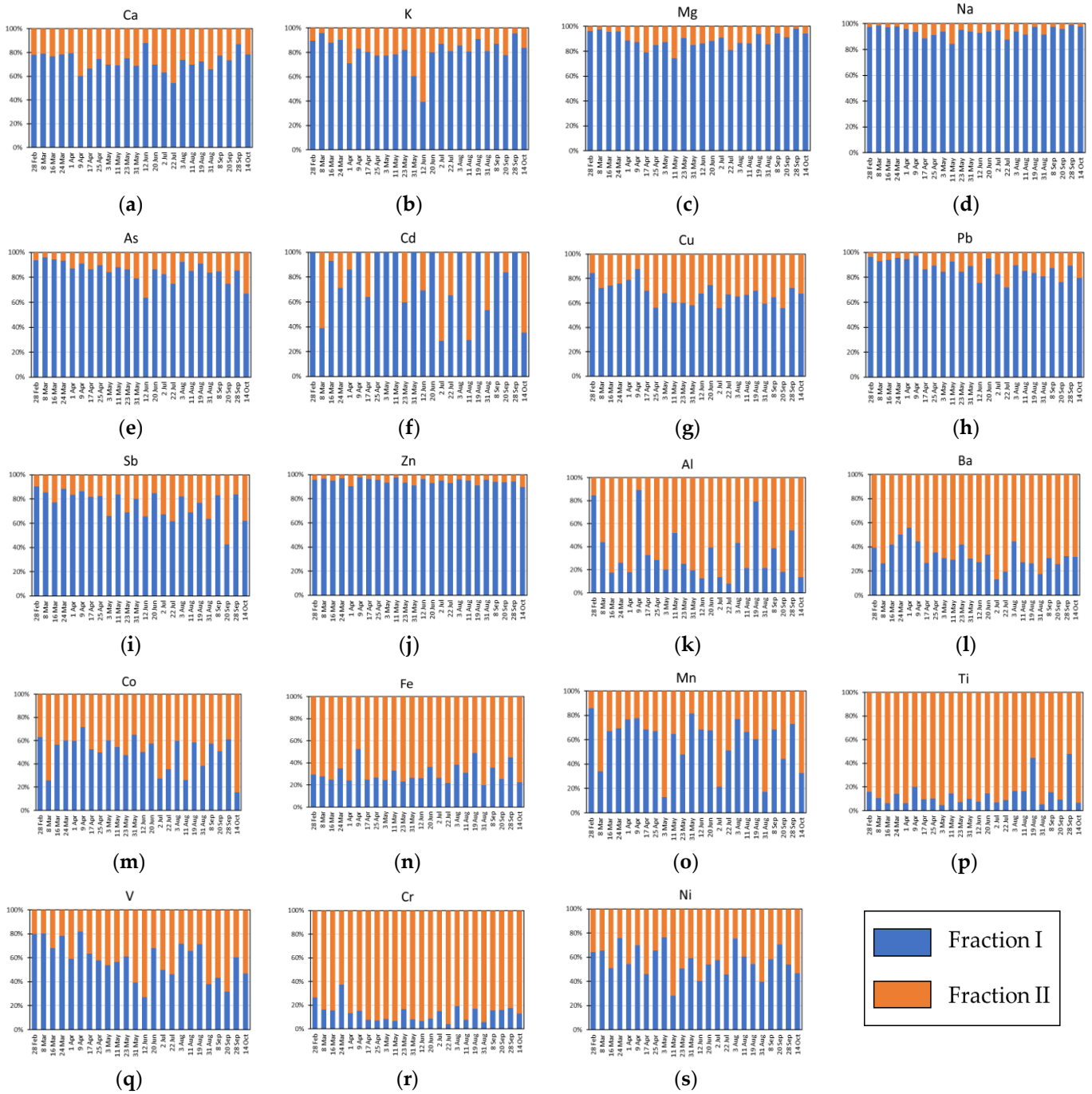

Figure 5. Extraction percentages obtained by means of the sequential extraction procedure on analytes prevalently having different origins: (**a**–**d**) marine; (**e**–**j**) anthropogenic; (**k**–**q**) crustal; (**r**,**s**) crustal from enriched soils of southwest Greenland.

Supplementary Figure S1 shows score and loading plots obtained by means of Principal Component Analysis on the results of the sequential extraction. All analytes have positive loadings on PC1 (representing the 39.37% of the total variance), therefore this PC allows to discriminate samples according to the extractability of all elements. In particular, the analytes having the highest loadings on PC1 are all anthropogenic and crustal elements

except Ti and Zn (namely Al, As, Ba, Cd, Co, Cu, Fe, Mn, Pb, Sb and V). By looking at the temporal trend of the PC1 scores shown in Figure 6, it is evident that the samples collected in late winter and early spring have positive scores, while the scores of the samples collected in late spring and early summer are mainly negative. However, in late summer and autumn there is a much higher variability since the scores are alternatively positive and negative.

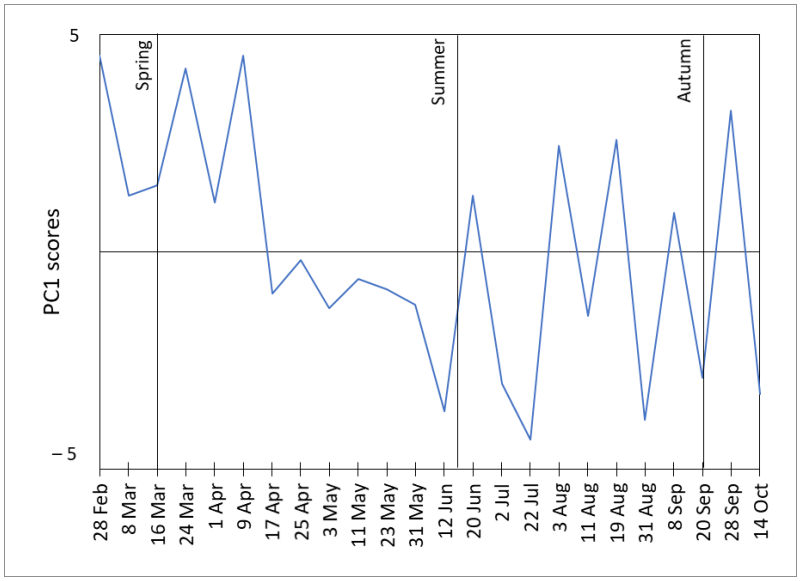

Figure 6. Temporal trend of the PC1 scores obtained by means of Principal Component Analysis on the results of the sequential extraction.

The observed temporal trend can be explained considering that, in winter and early spring, the long-range transport processes due to Arctic haze [38–40] strongly contribute to the Arctic airborne particulates. The air masses coming from mid-latitudes equivalently carry particles deriving from anthropogenic sources and particles deriving from rock erosion and soil resuspension of ice-free lands. The particles deriving from anthropogenic sources are generally small and can be easily transported. This causes not only an increase in the concentration of the above-mentioned analytes, but also an increase in their anthropogenic portion. Since the anthropogenic portion of each element is generally easily extractable [16,17], this also implies an increase of the extractability of these elements.

In contrast, only the smallest of the crustal particles can undergo such a long-range transport, thus causing a sort of size selection [3]. Considering that in winter and early spring the soil near to Ny-Ålesund is still completely covered by snow, the only crustal particles able to reach the sampling point in that season are the small particles travelling from mid-latitudes. This might easily explain the higher extractability of crustal elements in the samples collected at the beginning of the sampling campaign.

4. Conclusions

In this study, the source identification potential of a two-step sequential extraction procedure was evaluated and compared with the direct digestion of samples. For this purpose, the elemental composition of selected Arctic PM_{10} samples collected in Ny-Ålesund (Svalbard Islands) in 2015 was investigated. The multivariate analysis of the results obtained in this study, with the support of back-trajectory analyses, allowed to identify four main PM_{10} sources, namely marine, anthropogenic, crustal and Cr and Ni enriched-crustal, probably deriving from erosion of enriched soils of southwest Greenland. Moreover, a strong seasonal variation due to Arctic haze was evident. Even though the direct digestion of samples allowed a first source identification through CEFs and MEFs, the sequential extraction procedure provided a deeper comprehension of the specific sources

and the transport processes of PM from mid-latitudes. Indeed, it was possible to establish that most of the elements prevalently having an anthropogenic origin (As, Cd, Cu, Pb, Sb and Zn) were also less strongly bound to the particulate matter structure and, therefore, generally more easily releasable onto the Arctic snowpack. Moreover, in the samples collected in late winter and early spring, even the elements prevalently having a crustal origin were more easily extractable, probably due to the particle size selection occurred during the long-range transport. Finally, it was evident that the fraction more weakly bound to the atmospheric particulate solid phases (fraction I) increased when increasing concentrations of the elements were observed. As a whole, this study made it possible to understand that the soluble fraction of the elements present in the Arctic atmospheric particulate is generally high, and greater in the late winter and early spring than in other seasons; it is, therefore, evident that the application of a two-step sequential extraction procedure to Arctic PM samples can be a valid tool to better understand the complex phenomena occurring in the Arctic atmosphere and at air/snow/ocean interfaces.

Supplementary Materials: The following are available online at https://www.mdpi.com/article/10.3390/atmos12091152/s1, Table S1: Experimental conditions, limits of detection (LOD) and sample blanks (SB) of the analytes of interest with the technique used for their determination after direct digestion, Table S2: Experimental conditions, limits of detection (LOD) and sample blanks (SB) of the analytes of interest with the technique used for their determination in fraction I and fraction II, Table S3: Major element concentrations in Arctic PM_{10} samples collected in 2015. All the values are expressed in ng/m^3, Table S4: Minor and trace element concentrations in Arctic PM_{10} samples collected in 2015. All the values are expressed in pg/m^3, Table S5: Extraction percentages obtained for fraction I on the samples subjected to sequential extraction, Figure S1: Principal Component Analysis performed on the results of the sequential extraction: (a) score and (b) loading plot.

Author Contributions: Conceptualization, M.M. and R.T.; methodology, E.C., F.A. and M.M.; validation, E.C.; formal analysis, E.C.; investigation, E.C. and A.G. (Annapaola Giordano); resources, M.M., A.G. (Agnese Giacomino) and O.A.; data curation, E.C. and A.G. (Annapaola Giordano); writing—original draft preparation, E.C.; writing—review and editing, M.M., A.G. (Agnese Giacomino), P.I., F.A. and O.A.; visualization, E.C.; supervision, M.M.; project administration, M.M.; funding acquisition, M.M., R.T., A.G. (Agnese Giacomino) and O.A. All authors have read and agreed to the published version of the manuscript.

Funding: This research was funded by the Italian Ministry of Education, University and Research (PRIN no. 2007L8Y4NB_002 and no. 20092C7KRC_002).

Institutional Review Board Statement: Not applicable.

Informed Consent Statement: Not applicable.

Acknowledgments: The authors thank CNR and its local staff for the logistic support that allowed the realization of the experimental activity and Mauro Mazzola of CNR-ISP for providing the HYSPLIT outputs used in this study.

Conflicts of Interest: The authors declare no conflict of interest. The funders had no role in the design of the study; in the collection, analyses, or interpretation of data; in the writing of the manuscript, or in the decision to publish the results.

References

1. Serreze, M.C.; Barry, R.G. Processes and impacts of Arctic amplification: A research synthesis. *Glob. Planet. Chang.* **2011**, *77*, 85–96. [CrossRef]
2. Maturilli, M.; Hanssen-Bauer, I.; Neuber, R.; Rex, M.; Edvardsen, K. The Atmosphere Above Ny-Ålesund: Climate and Global Warming, Ozone and Surface UV Radiation. In *The Ecosystem of Kongsfjorden, Svalbard*; Springer: Cham, Switzerland, 2019; pp. 23–46, ISBN 978-3-319-46425-1.
3. Giardi, F.; Traversi, R.; Becagli, S.; Severi, M.; Caiazzo, L.; Ancillotti, C.; Udisti, R. Determination of Rare Earth Elements in multi-year high-resolution Arctic aerosol record by double focusing Inductively Coupled Plasma Mass Spectrometry with desolvation nebulizer inlet system. *Sci. Total Environ.* **2018**, *613–614*, 1284–1294. [CrossRef] [PubMed]
4. Cappelletti, D.; Azzolini, R.; Langone, L.; Ventura, S.; Viola, A.; Aliani, S.; Vitale, V.; Brugnoli, E. Environmental changes in the Arctic: An Italian perspective. *Rend. Fis. Acc. Lincei* **2016**, *27*, S1–S6. [CrossRef]

5. Becagli, S.; Caiazzo, L.; Di Iorio, T.; di Sarra, A.; Meloni, D.; Muscari, G.; Pace, G.; Severi, M.; Traversi, R. New insights on metals in the Arctic aerosol in a climate changing world. *Sci. Total Environ.* **2020**, *741*, 1–9. [CrossRef]
6. Barbaro, E.; Zangrando, R.; Kirchgeorg, T.; Bazzano, A.; Illuminati, S.; Annibaldi, A.; Rella, S.; Truzzi, C.; Grotti, M.; Ceccarini, A.; et al. An integrated study of the chemical composition of Antarctic aerosol to investigate natural and anthropogenic sources. *Environ. Chem.* **2016**, *13*, 867–876. [CrossRef]
7. Bazzano, A.; Soggia, F.; Grotti, M. Source identification of atmospheric particle-bound metals at Terra Nova Bay, Antarctica. *Environ. Chem.* **2015**, *12*, 245–252. [CrossRef]
8. Conca, E.; Abollino, O.; Giacomino, A.; Buoso, S.; Traversi, R.; Becagli, S.; Grotti, M.; Malandrino, M. Source identification and temporal evolution of trace elements in PM10 collected near to Ny-Ålesund (Norwegian Arctic). *Atmos. Environ.* **2019**, *203*, 153–165. [CrossRef]
9. Bazzano, A.; Ardini, F.; Grotti, M.; Malandrino, M.; Giacomino, A.; Abollino, O.; Cappelletti, D.; Becagli, S.; Traversi, R.; Udisti, R. Elemental and lead isotopic composition of atmospheric particulate measured in the Arctic region (Ny-Ålesund, Svalbard Islands). *Rend. Lincei Sci. Fis. Nat.* **2016**, *27*, S73–S84. [CrossRef]
10. Annibaldi, A.; Truzzi, C.; Illuminati, S.; Bassotti, E.; Scarponi, G. Determination of water-soluble and insoluble (dilute-HCl-extractable) fractions of Cd, Pb and Cu in Antarctic aerosol by square wave anodic stripping voltammetry: Distribution and summer seasonal evolution at Terra Nova Bay (Victoria Land). *Anal. Bioanal. Chem.* **2007**, *387*, 977–998. [CrossRef]
11. Canepari, S.; Perrino, C.; Olivieri, F.; Astolfi, M.L. Characterisation of the traffic sources of PM through size-segregated sampling, sequential leaching and ICP analysis. *Atmos. Environ.* **2008**, *42*, 8161–8175. [CrossRef]
12. Canepari, S.; Astolfi, M.L.; Moretti, S.; Curini, R. Comparison of extracting solutions for elemental fractionation in airborne particulate matter. *Talanta* **2010**, *82*, 834–844. [CrossRef]
13. Illuminati, S.; Annibaldi, A.; Truzzi, C.; Libani, G.; Mantini, C.; Scarponi, G. Determination of water-soluble, acid-extractable and inert fractions of Cd, Pb and Cu in Antarctic aerosol by square wave anodic stripping voltammetry after sequential extraction and microwave digestion. *J. Electroanal. Chem.* **2015**, *755*, 182–196. [CrossRef]
14. Truzzi, C.; Annibaldi, A.; Illuminati, S.; Mantini, C.; Scarponi, G. Chemical fractionation by sequential extraction of Cd, Pb, and Cu in Antarctic atmospheric particulate for the characterization of aerosol composition, sources, and summer evolution at Terra Nova Bay, Victoria Land. *Air Qual. Atmos. Health* **2017**, *10*, 783–798. [CrossRef]
15. Bacon, J.R.; Davidson, C.M. Is there a future for sequential chemical extraction? *Analyst* **2008**, *133*, 25–46. [CrossRef]
16. Kyotani, T.; Iwatsuki, M. Characterization of soluble and insoluble components in PM2.5 and PM10 fractions of airborne particulate matter in Kofu city, Japan. *Atmos. Environ.* **2002**, *36*, 639–649. [CrossRef]
17. Gouws, K.; Coetzee, P.P. Determination and partitioning of heavy metals in sediments of the Vaal Dam System by sequential extraction. *Water SA* **1997**, *23*, 217–226.
18. Voutsa, D.; Samara, C. Labile and bioaccessible fractions of heavy metals in the airborne particulate matter from urban and industrial areas. *Atmos. Environ.* **2002**, *36*, 3583–3590. [CrossRef]
19. Karthikeyan, S.; Joshi, U.M.; Balasubramanian, R. Microwave assisted sample preparation for determining water-soluble fraction of trace elements in urban airborne particulate matter: Evaluation of bioavailability. *Anal. Chim. Acta* **2006**, *576*, 23–30. [CrossRef]
20. Limbeck, A.; Wagner, C.; Lendl, B.; Mukhtar, A. Determination of water soluble trace metals in airborne particulate matter using a dynamic extraction procedure with on-line inductively coupled plasma optical emission spectrometric detection. *Anal. Chim. Acta* **2012**, *750*, 111–119. [CrossRef]
21. Conca, E.; Malandrino, M.; Giacomino, A.; Costa, E.; Ardini, F.; Inaudi, P.; Abollino, O. Optimization of a sequential extraction procedure for trace elements in Arctic PM10. *Anal. Bioanal. Chem.* **2020**, *412*, 7429–7440. [CrossRef]
22. Mazzola, M.; Viola, A.; Lanconelli, C.; Vitale, V. Atmospheric observations at the Amundsen-Nobile Climate Change Tower in Ny-Ålesund, Svalbard. *Rend. Lincei Sci. Fis. Nat.* **2016**, *27*, 7–18. [CrossRef]
23. Nóbrega, J.A.; Pirola, C.; Richter, R.C. *Think Blank. Clean Chemistry Tools for Atomic Spectroscopy*; Milestone Srl and Ikonos Srl: Sorisole, Italy, 2017.
24. Conca, E.; Malandrino, M.; Giacomino, A.; Buoso, S.; Berto, S.; Verplanck, P.L.; Magi, E.; Abollino, O. Dynamics of inorganic components in lake waters from Terra Nova Bay, Antarctica. *Chemosphere* **2017**, *183*, 454–470. [CrossRef] [PubMed]
25. Krnavek, L.; Simpson, W.R.; Carlson, D.; Domine, F.; Douglas, T.; Sturm, M. The chemical composition of surface snow in the Arctic: Examining marine, terrestrial, and atmospheric influences. *Atmos. Environ.* **2012**, *50*, 349–359. [CrossRef]
26. Tahri, M.; Benchrif, A.; Bounakhla, M.; Benyaich, F.; Noack, Y. Seasonal variation and risk assessment of PM2.5 and PM2.5-10 in the ambient air of Kenitra, Morocco. *Environ. Sci. Process. Impacts* **2017**, *19*, 1427–1436. [CrossRef]
27. Wedepohl, K.H. The composition of the continental crust. *Geochim. Cosmochim. Acta* **1995**, *59*, 1217–1232. [CrossRef]
28. Goldberg, E.D. Chapter 5: Minor elements in sea water. In *Chemical Oceanography*; Riley, J.P., Skirrow, G., Eds.; Academic Press: London, UK, 1965; pp. 163–196.
29. Einax, W.; Zwanziger, H.W.; Gei, S. *Chemometrics in Environmental Analysis*; Wiley-VHC: Weinhem, Germany, 1997.
30. Massart, D.L.; Vandenginste, B.G.M.; Buydens, L.M.C.; De Jono, S.; Leqi, P.J.; Smeyers-Verbeke, J. *Handbook of Chemometrics and Qualimetrics, Parts A and B*; Elsevier: Amsterdam, The Netherlands, 1997.
31. Ruxton, G.D.; Beauchamp, G. Some suggestions about appropriate use of the Kruskal-Wallis test. *Anim. Behav.* **2008**, *76*, 1083–1087. [CrossRef]

32. Draxler, R.R.; Rolph, G.D. HYSPLIT (HYbrid Single-Particle Lagrangian Integrated Trajectory) Model Access via NOAA ARL READY. Available online: http://ready.arl.noaa.gov/HYSPLIT.php (accessed on 22 July 2021).
33. Stein, A.F.; Draxler, R.R.; Rolph, G.D.; Stunder, B.J.B.; Cohen, M.D.; Ngan, F. NOAA's HYSPLIT atmospheric transport and dispersion modeling system. *Bull. Am. Meteorol. Soc.* **2015**, *96*, 2059–2077. [CrossRef]
34. Lai, A.M.; Shafer, M.M.; Dibb, J.E.; Polashenski, C.M.; Schauer, J.J. Elements and inorganic ions as source tracers in recent Greenland snow. *Atmos. Environ.* **2017**, *164*, 205–215. [CrossRef]
35. Zajusz-Zubek, E.; Radko, T.; Mainka, A. Fractionation of trace elements and human health risk of submicron particulate matter (PM1) collected in the surroundings of coking plants. *Environ. Monit. Assess.* **2017**, *189*, 389. [CrossRef] [PubMed]
36. Moroni, B.; Cappelletti, D.; Ferrero, L.; Crocchianti, S.; Busetto, M.; Mazzola, M.; Becagli, S.; Traversi, R.; Udisti, R. Local vs long-range sources of aerosol particles upon Ny-Ålesund (Svalbard Islands): Mineral chemistry and geochemical records. *Rend. Lincei Sci. Fis. Nat.* **2016**, *27*, S115–S127. [CrossRef]
37. Wager, L.R.; Mitchell, R.L. The distribution of trace elements during strong fractionation of basic magma—A further study of the Skaergaard intrusion, East Greenland. *Geochim. Cosmochim. Acta* **1951**, *1*, 129–208. [CrossRef]
38. Lupi, A.; Busetto, M.; Becagli, S.; Giardi, F.; Lanconelli, C.; Mazzola, M.; Udisti, R.; Hansson, H.C.; Henning, T.; Petkov, B.; et al. Multi-seasonal ultrafine aerosol particle number concentration measurements at the Gruvebadet observatory, Ny-Ålesund, Svalbard Islands. *Rend. Lincei Sci. Fis. Nat.* **2016**, *27*, S59–S71. [CrossRef]
39. Udisti, R.; Bazzano, A.; Becagli, S.; Bolzacchini, E.; Caiazzo, L.; Cappelletti, D.; Ferrero, L.; Frosini, D.; Giardi, F.; Grotti, M.; et al. Sulfate source apportionment in the Ny-Ålesund (Svalbard Islands) Arctic aerosol. *Rend. Lincei Sci. Fis. Nat.* **2016**, *27*, S85–S94. [CrossRef]
40. Quinn, P.K.; Shaw, G.E.; Andrews, E.; Dutton, E.G.; Ruoho-Airola, T.; Gong, S.L. Arctic haze: Current trends and knowledge gaps. *Tellus B* **2007**, *59*, 99–114. [CrossRef]

Supplementary Table S1. Experimental conditions, limits of detection (LOD) and sample blanks (SB) of the analytes of interest with the technique used for their determination after direct digestion.

SF-ICP-MS				
	Isotope	**Resolution**	**LOD (ng/L)**	**SB (µg/L)**
Al	27	LR-MR	400	0.63
As	75	MR	42	< LOD
Ba	135-137-138	LR-MR	300	62
Cd	111-112-114	LR	2.3	< LOD
Co	59	LR-MR	1.9	< LOD
Cr	53	MR	10	< LOD
Cu	63-65	LR-MR	11	< LOD
Fe	56-57	MR	400	3.2
Mn	55	LR-MR	8.6	0.04
Ni	60-61-62	LR-MR	45	0.5
Pb	206-207-208	LR-MR	40	0.23
Sb	121-123	MR	23	< LOD
Ti	46-47-48	LR-MR	750	< LOD
V	51	LR-MR	58	< LOD
Zn	66-68	LR-MR	190	4.5

ICP-OES			
	λ (nm)	**LOD (µg/L)**	**SB (µg/L)**
Ca	317.93	3.1	260
K	769.90	1.5	8.8
Mg	285.21	1.2	< LOD
Na	589.59	11	210

LR = low resolution; MR = medium resolution

Supplementary Table S2. Experimental conditions, limits of detection (LOD) and sample blanks (SB) of the analytes of interest with the technique used for their determination in fraction I and fraction II.

Fraction I					Fraction II				
SF-ICP-MS					SF-ICP-MS				
	Isotope	Resolution	LOD (ng/L)	SB (μg/L)		Isotope	Resolution	LOD (ng/L)	SB (μg/L)
Al	27	LR-MR	250	8.2	**Al**	27	LR-MR	400	40
As	75	MR	3.4	0.02	**As**	75	MR	42	< LOD
Ba	135-137-138	LR-MR	120	0.2	**Ba**	135-137-138	LR-MR	300	1.5
Cd	111-112-114	LR	12	< LOD	**Cd**	111-112-114	LR	2.3	0.03
Co	59	LR-MR	8	< LOD	**Co**	59	LR-MR	1.9	0.02
Cr	53	MR	30	0.08	**Cr**	53	MR	10	0.05
Cu	63-65	LR-MR	42	0.21	**Cu**	63-65	LR-MR	11	0.35
Fe	56-57	MR	430	2.3	**Fe**	56-57	MR	400	34
Mn	55	LR-MR	45	0.13	**Mn**	55	LR-MR	8.6	0.7
Ni	60-61-62	LR-MR	83	1.3	**Ni**	60-61-62	LR-MR	45	0.5
Pb	206-207-208	LR-MR	24	0.62	**Pb**	206-207-208	LR-MR	40	0.35
Sb	121-123	MR	23	0.13	**Sb**	121-123	MR	23	< LOD
Ti	46-47-48	LR-MR	50	0.20	**Ti**	46-47-48	LR-MR	750	1.2
V	51	LR-MR	10	< LOD	**V**	51	LR-MR	58	< LOD
Zn	66-68	LR-MR	160	9.4	**Zn**	66-68	LR-MR	190	5.2

Fraction I			
ICP-OES			
	λ (nm)	LOD (μg/L)	SB (μg/L)
Ca	317.93	8.5	60
K	769.90	4.5	17
Mg	285.21	3.0	8.7
Na	589.59	3.3	126
Zn	213.86	0.7	9.4

Fraction II			
ICP-OES			
	λ (nm)	LOD (μg/L)	SB (μg/L)
Ca	317.93	3.1	168
K	769.90	1.5	15
Mg	285.21	1.2	12
Na	589.59	11	80
Zn	213.86	1.0	5.2

LR = low resolution; MR = medium resolution

Supplementary Table S3. Major element concentrations in Arctic PM_{10} samples collected in 2015. All the values are expressed in ng/m^3.

Sampling start date	Al	Ca	Fe	K	Mg	Na	Sampling start date	Al	Ca	Fe	K	Mg	Na
28th February	6.96 ± 0.05	26.6 ± 0.6	5.8 ± 0.1	19.0 ± 0.5	70.6 ± 0.6	478 ± 5	24th June	2.08 ± 0.02	10.9 ± 0.2	2.55 ± 0.04	4.50 ± 0.09	10.3 ± 0.2	74 ± 1
4th March	0.36 ± 0.01	6.96 ± 0.02	0.67 ± 0.02	5.78 ± 0.09	21.8 ± 0.1	168 ± 1	28th June	2.08 ± 0.08	12.9 ± 0.4	2.17 ±0.06	6.0 ± 0.2	18.9 ± 0.3	144 ± 1
8th March	1.77 ± 0.05	28.5 ± 0.7	2.4 ± 0.1	21.1 ± 0.1	79 ± 1	599 ± 9	2nd July	0.64 ± 0.02	13.9 ± 0.2	1.02 ± 0.03	8.72 ± 0.08	26 ± 1	208 ± 2
12th March	5.3 ± 0.2	38.3 ± 0.9	8.06 ± 0.09	33 ±1	109 ± 2	858 ± 27	6th July	3.56 ± 0.04	13.4 ± 0.2	3.83 ± 0.06	5.1 ± 0.2	12.4 ± 0.1	88.8 ± 0.8
16th March	7.7 ± 0.2	39.8 ± 0.9	5.61 ± 0.06	27.4 ± 0.8	90 ± 2	573 ± 9	10th July	27.1 ± 0.3	17.0 ± 0.2	7.6 ± 0.1	19.8 ± 0.1	11.0 ± 0.3	63.8 ± 0.5
20th March	8.2 ± 0.1	9.5 ± 0.3	5.7 ± 0.1	5.1 ± 0.1	12.7 ± 0.1	71.0 ± 0.8	14th July	4.28 ± 0.09	9.37 ± 0.04	2.21 ± 0.06	< 1.98	4.16 ± 0.04	24.6 ± 0.3
24th March	4.5 ± 0.1	13.7 ± 0.3	3.94 ± 0.05	12.2 ± 0.2	40.3 ± 0.2	342 ± 4	18th July	1.19 ± 0.01	5.3 ± 0.1	0.63 ± 0.01	2.94 ± 0.02	2.31 ± 0.04	31.5 ± 0.5
28th March	3.3 ± 0.1	18.8 ± 0.7	2.9 ± 0.1	12.3 ± 0.1	46.7 ± 0.9	325 ± 4	22nd July	1.27 ± 0.02	12.33 ± 0.08	1.63 ± 0.03	5.83 ± 0.01	20.0 ± 0.1	171 ± 3
1st April	30.8 ± 0.4	28.6 ± 0.9	19.5 ± 0.1	18.5 ± 0.5	42 ± 1	238 ± 3	26th July	1.15 ± 0.02	10.01 ± 0.07	1.98 ± 0.03	4.4 ± 0.1	14.3 ± 0.3	104 ± 1
5th April	28.1 ± 0.8	49.7 ± 0.6	22.3 ± 0.1	19.1 ± 0.1	41.3 ± 0.6	220 ± 3	30th July	7.45 ± 0.05	9.7 ± 0.1	5.16 ± 0.09	3.94 ± 0.07	5.06 ± 0.09	27.3 ± 0.1
9th April	5.46 ± 0.09	8.1 ± 0.1	5.3 ± 0.1	6.0 ± 0.2	9.3 ± 0.3	61 ± 1	3rd August	5.55 ± 0.08	15.8 ± 0.2	4.4 ± 0.1	10.8 ± 0.1	23.3 ± 0.3	171 ± 1
13th April	9.1 ± 0.2	27.2 ± 0.4	8.0 ± 0.1	21.0 ± 0.1	66 ± 2	500 ± 1	7th August	1.38 ± 0.01	6.1 ± 0.3	1.13 ± 0.02	2.89 ± 0.07	4.91 ± 0.05	41.8 ± 0.3
17th April	2.5 ± 0.1	3.85 ± 0.06	1.8 ± 0.1	2.71 ± 0.02	8.0 ± 0.1	59.8 ± 0.2	11th August	3.0 ± 0.1	10.5 ± 0.3	2.18 ± 0.08	3.56 ± 0.03	8.71 ± 0.09	55 ± 1
21st April	3.3 ± 0.1	6.1 ± 0.1	2.50 ± 0.08	3.7 ± 0.1	12.8 ± 0.3	84.6 ± 0.1	15th August	2.04 ± 0.05	10.5 ± 0.1	2.01 ± 0.04	7.4 ± 0.1	21.9 ± 0.5	187 ± 2
25th April	4.46 ± 0.07	11.57 ± 0.08	3.22 ± 0.05	4.08 ± 0.07	11.7 ± 0.1	75 ± 1	19th August	0.95 ± 0.01	10.3 ± 0.3	1.55 ± 0.03	6.7 ± 0.1	22.6 ± 0.4	195 ± 1
29th April	6.63 ± 0.06	16.7 ± 0.2	4.97 ± 0.08	4.9 ±0.1	10.9 ± 0.1	61 ± 1	23th August	1.09 ± 0.05	5.21 ± 0.08	1.18 ± 0.04	2.99 ± 0.05	5.5 ± 0.1	47 ± 1
3rd May	4.59 ± 0.07	15.0 ± 0.2	3.47 ± 0.05	5.4 ± 0.2	17.9 ± 0.2	125 ± 1	27th August	0.90 ± 0.01	3.64 ± 0.07	0.78 ± 0.01	2.44 ± 0.08	3.4 ± 0.1	32.3 ± 0.3
7th May	9.3 ± 0.1	14.69 ± 0.06	5.0 ± 0.1	5.85 ± 0.06	16.3 ± 0.1	112 ± 1	31st August	1.06 ± 0.03	8.0 ± 0.1	0.99 ± 0.03	2.39 ± 0.03	9.04 ± 0.09	63 ± 1
11th May	1.86 ± 0.07	8.6 ± 0.1	1.43 ± 0.06	2.92 ± 0.05	7.0 ± 0.1	45.2 ± 0.7	4th September	0.95 ± 0.02	10.1 ± 0.2	1.14 ± 0.02	4.5 ± 0.1	14.5 ± 0.2	112 ± 1
15th May	1.02 ± 0.02	7.01 ± 0.08	0.91 ± 0.01	2.66 ± 0.03	9.45 ± 0.05	71.5 ± 0.5	8th September	9.8 ± 0.1	28.0 ± 0.5	7.5 ± 0.1	14.1 ± 0.2	50.4 ± 0.4	370 ± 3
19th May	3.62 ± 0.06	17.4 ± 0.1	2.80 ± 0.05	10.8 ± 0.1	36.0 ± 0.1	270 ± 3	12th September	2.39 ± 0.04	14.1 ± 0.1	2.42 ± 0.05	9.5 ± 0.1	27.8 ± 0.4	233 ± 1
23rd May	4.42 ± 0.05	17.3 ± 0.6	3.32 ± 0.04	8.80 ± 0.08	29.3 ± 0.2	213 ± 3	16th September	18.9 ± 0.5	69 ± 2	16.9 ± 0.4	52.8 ± 0.3	162 ± 3	1242 ± 1
27th May	6.9 ± 0.2	12.57 ± 0.06	4.57 ± 0.07	5.81 ± 0.07	15.5 ± 0.2	118 ± 2	20th September	5.96 ± 0.04	14.3 ± 0.2	4.75 ± 0.06	7.4 ± 0.2	19.1 ± 0.6	141 ± 1
31st May	7.2 ± 0.2	10.5 ± 0.2	7.6 ± 0.4	5.7 ± 0.1	11.9 ± 0.2	74 ±1	24th September	0.59 ± 0.01	7.04 ± 0.06	0.33 ± 0.01	2.56 ± 0.02	10.4 ± 0.1	75.9 ±0.4
4th June	2.04 ± 0.04	14.68 ± 0.07	2.34 ± 0.05	9.1 ± 0.2	31.8 ± 0.7	243 ± 1	28th September	4.5 ± 0.1	40.6 ± 0.9	4.03 ± 0.09	28.3 ± 0.1	95 ± 1	838 ± 7
8th June	8.6 ± 0.1	20.5 ± 0.3	7.1 ± 0.1	7.8 ± 0.2	21.8 ± 0.8	139 ± 1	2nd October	11.6 ± 0.2	19.9 ± 0.8	9.3 ± 0.2	7.1 ± 0.3	15.1 ± 0.4	73.8 ± 0.8
12th June	20.6 ± 0.1	55 ± 2	18.4 ± 0.5	14.4 ± 0.2	40.5 ± 0.8	184 ± 4	6th October	1.54 ± 0.08	26.0 ± 0.9	1.57 ± 0.06	20.2 ± 0.4	73.9 ± 0.6	619 ± 1
16th June	4.9 ± 0.1	12.5 ± 0.1	2.28 ± 0.05	7.4 ± 0.1	24.5 ± 0.3	189 ± 2	14th October	7.7 ± 0.2	19.5 ± 0.5	7.5 ± 0.1	12.0 ± 0.4	37.5 ± 0.4	306 ± 6
20th June	0.88 ± 0.01	13.9 ± 0.3	1.45 ± 0.02	4.27 ± 0.08	12.2 ± 0.3	83 ±1	18th October	2.05 ± 0.06	9.34 ± 0.03	1.93 ± 0.03	4.6 ± 0.1	14.0 ± 0.1	107 ± 2

Supplementary Table S4. Minor and trace element concentrations in Arctic PM_{10} samples collected in 2015. All the values are expressed in pg/m^3.

Sampling start date	As	Ba	Cd	Co	Cr	Cu	Mn	Ni	Pb	Sb	Ti	V	Zn
28th February	33 ± 1	74 ± 3	5.5 ± 0.4	7.20 ± 0.07	284 ± 9	92 ± 3	214 ± 4	170 ± 10	146 ± 4	12.7 ± 0.7	220 ± 10	27.3 ± 0.8	310 ± 10
4th March	8.4 ± 0.2	13.1 ± 0.8	0.96 ± 0.01	0.70 ± 0.03	19.2 ±0.7	11 ± 1	19.2 ± 0.3	25 ± 1	38.5 ± 0.9	2.61 ± 0.04	29.2 ± 0.7	3.5 ± 0.1	35 ± 2
8th March	42 ± 1	29 ± 1	4.1 ± 0.3	1.6 ± 0.1	76 ± 4	35 ± 1	56 ± 1	37 ± 1	90 ± 2	12.7 ± 0.2	650 ± 20	14.4 ± 0.7	350 ± 20
12th March	149 ± 7	81 ± 2	27 ± 1	5.7 ± 0.2	84 ± 2	113 ± 2	240 ± 10	59 ± 3	500 ± 20	29.3 ± 0.9	298 ± 9	32.6 ± 0.3	1,040 ± 30
16th March	75 ± 4	118 ± 3	12.6 ± 0.5	6.5 ± 0.2	35 ± 1	90 ± 2	208 ± 5	52 ± 3	342 ± 5	24.5 ± 0.4	365 ± 7	27.4 ± 0.3	790 ± 10
20th March	47.0 ± 0.6	124 ± 4	8.3 ± 0.2	4.8 ± 0.2	51 ± 1	40 ± 1	184 ± 4	36 ± 1	268 ± 5	19.9 ± 0.4	370 ± 10	27.1 ± 0.8	351 ± 8
24th March	31 ± 2	92 ± 2	5.4 ± 0.2	3.3 ± 0.1	32 ± 2	52 ± 2	140 ± 9	48 ± 1	202 ± 6	19.1 ± 0.3	300 ± 10	32.0 ± 0.5	330 ± 10
28th March	22.0 ± 0.6	62 ± 2	3.26 ± 0.09	1.97 ± 0.08	22 ± 1	30 ± 1	103 ± 3	18 ± 1	100 ± 2	13.3 ± 0.2	175 ± 3	20 ± 1	160 ± 5
1st April	73 ± 7	336 ± 6	10.7 ± 0.6	12.8 ± 0.8	85 ± 2	103 ± 3	627 ± 9	69 ± 5	320 ± 6	24.1 ± 0.8	1,250 ±10	75 ± 2	600 ± 20
5th April	369 ± 11	323 ± 6	45 ± 1	17 ± 1	134 ± 7	280 ± 10	870 ± 20	133 ± 5	1,160 ± 20	56 ± 1	1,190 ± 10	127 ± 3	2,600 ± 100
9th April	84 ± 4	77 ± 3	13.7 ± 0.4	4.2 ± 0.1	103 ± 4	121 ± 3	165 ± 2	66 ± 4	485 ± 4	31.4 ± 0.5	256 ± 7	36.6 ± 0.5	690 ± 30
13th April	21 ± 1	96 ± 3	2.7 ± 0.2	9.8 ± 0.2	92 ± 3	49 ± 1	1,270 ± 50	149 ± 4	87 ± 2	12.5 ± 0.3	410 ± 10	28 ± 1	190 ± 6
17th April	13.9 ± 0.3	28 ± 1	2.1 ± 0.1	0.84 ± 0.02	20.7 ± 0.9	7.9 ± 0.4	53 ± 2	24 ± 1	56 ± 1	9.2 ± 0.3	102 ± 6	7.1 ± 0.3	105 ± 4
21st April	13.5 ± 0.7	46 ± 1	2.3 ± 0.1	1.6 ± 0.1	11.0 ± 0.6	16.0 ± 0.8	69 ± 1	13.2 ± 0.9	43 ± 1	9.8 ± 0.2	195 ± 5	8.0 ± 0.5	101 ± 4
25th April	11.9 ± 0.6	49 ± 1	2.14 ± 0.08	2.0 ± 0.1	21.6 ± 0.7	13.9 ± 0.4	86.9 ± 0.5	22 ± 1	53.1 ± 0.5	6.2 ± 0.1	192 ± 3	10.6 ± 0.5	85 ± 3
29th April	14.7 ± 0.3	71 ± 3	2.1 ± 0.2	2.7 ± 0.2	17 ± 1	17 ± 1	143 ± 3	18.6 ± 0.7	59 ± 2	6.4 ± 0.2	230 ± 10	20.9 ± 0.7	127 ± 8
3rd May	11.9 ± 0.6	53 ± 1	1.69 ± 0.08	1.5 ± 0.1	17.1 ± 0.3	15.8 ± 0.9	116 ± 5	17.4 ± 0.7	43 ± 1	6.3 ± 0.2	213 ± 4	14.1 ± 0.1	132 ± 4
7th May	10.7 ± 0.8	64 ± 2	1.56 ± 0.07	3.26 ± 0.01	39 ± 1	17.4 ± 0.9	155 ± 1	38 ± 3	37 ± 1	3.4 ± 0.1	380 ± 7	18.5 ± 0.7	113 ± 4
11th May	4.7 ± 0.2	32 ± 2	1.14 ± 0.06	0.89 ± 0.05	1.30 ± 0.06	3.8 ± 0.3	53 ± 2	6.2 ± 0.2	25.4 ± 0.8	3.3 ± 0.2	80 ± 2	5.7 ± 0.2	37 ± 2
15th May	3.7 ± 0.4	14.2 ± 0.5	0.60 ± 0.01	0.50 ± 0.02	7.6 ± 0.2	249 ± 4	26.5 ± 0.5	7.7 ± 0.3	10.2 ± 0.2	2.6 ± 0.1	69.0 ± 0.8	2.39 ± 0.09	46 ± 2
19th May	10.9 ± 0.6	41 ± 1	1.54 ± 0.07	1.51 ± 0.06	19.7 ± 0.4	9.6 ± 0.6	83 ± 2	17 ± 1	40 ± 1	5.3 ± 0.2	167 ± 7	12.3 ± 0.4	89 ± 3
23rd May	15.7 ± 0.4	62 ± 2	2.41 ± 0.02	2.1 ± 0.1	39 ± 2	12.2 ± 0.3	124 ± 4	24 ± 2	51.3 ± 0.6	8.7 ± 0.3	233 ± 6	11.5 ± 0.4	149 ± 8
27th May	11.3 ± 0.9	67 ± 4	2.06 ± 0.05	2.7 ± 0.2	6.8 ± 0.4	9.1 ± 0.3	139 ± 5	22 ± 1	40 ± 2	6.01 ± 0.07	333 ± 6	15.0 ± 0.6	117 ± 5
31st May	8.5 ± 0.6	105 ± 3	0.94 ± 0.08	6.1 ± 0.2	172 ± 8	18.9 ± 0.9	360 ± 20	95 ± 5	25.2 ± 0.5	4.0 ± 0.2	330 ± 10	16.2 ± 0.6	61 ± 6
4th June	3.6 ± 0.2	36 ± 2	< 0.37	1.2 ± 0.1	n.a.	40 ± 3	113 ± 1	10.7 ± 0.7	8.6 ± 0.3	n.a.	107 ± 6	3.4 ± 0.2	19 ± 1
8th June	7.5 ± 0.4	102 ± 4	1.08 ± 0.05	4.7 ± 0.2	12.1 ± 0.7	9.1 ± 0.6	251 ± 6	19 ± 1	16.5 ± 0.3	2.34 ± 0.05	393 ± 6	20.3 ± 0.5	50 ± 1
12th June	10.1 ± 0.5	237 ± 7	0.380 ± 0.005	9.2 ± 0.5	33 ± 1	43 ± 2	530 ± 20	46 ± 3	23.0 ± 0.5	2.8 ± 0.2	790 ± 20	36.8 ± 0.9	51 ± 2
16th June	5.9 ± 0.2	32 ± 2	1.00 ± 0.06	2.17 ± 0.07	29 ± 2	46 ± 3	95 ± 2	48 ± 1	18 ± 1	3.15 ± 0.05	203 ± 2	12.2 ± 0.3	37 ± 2
20th June	10.1 ± 0.7	24 ± 1	0.56 ± 0.03	1.02 ± 0.07	13.6 ± 0.6	122 ± 2	44 ± 1	85 ± 4	29.9 ± 0.5	3.5 ± 0.1	< 7.9	5.5 ± 0.4	440 ± 20

continued

Sampling start date	As	Ba	Cd	Co	Cr	Cu	Mn	Ni	Pb	Sb	Ti	V	Zn
24th June	4.98 ± 0.08	32 ± 1	0.39 ± 0.01	1.9 ± 0.2	41 ± 2	19.2 ± 0.6	93 ± 3	29 ± 1	12.9 ± 0.4	2.89 ± 0.09	66 ± 2	17 ± 1	70 ± 4
28th June	4.8 ± 0.3	29 ± 1	0.47 ± 0.02	1.24 ± 0.07	55 ± 2	65 ± 2	49 ± 1	13.6 ± 0.7	10.7 ± 0.3	3.05 ± 0.09	102 ± 1	6.8 ± 0.4	67 ± 4
2nd July	3.73 ± 0.06	12.6 ± 0.3	0.58 ± 0.04	0.80 ± 0.03	15.7 ± 0.7	2.5 ± 0.2	27.2 ± 0.1	13.9 ± 0.4	4.63 ± 0.06	2.26 ± 0.06	53.8 ± 0.8	3.7 ± 0.2	30 ± 2
6th July	6.2 ± 0.2	45 ± 2	0.57 ± 0.03	3.6 ± 0.3	15.1 ± 0.5	66 ± 1	184 ± 9	15.7 ± 0.7	10.1 ± 0.2	2.22 ± 0.08	179 ± 6	7.8 ± 0.3	76 ± 3
10th July	33 ± 2	156 ± 4	12.5 ± 0.4	4.59 ± 0.09	69 ± 2	72 ± 1	440 ± 10	97 ± 4	38 ± 1	3.95 ± 0.09	470 ± 10	90 ± 1	1,160 ± 20
14th July	3.74 ± 0.07	53 ± 2	< 0.35	1.29 ± 0.08	33 ± 1	8.7 ± 0.3	81 ± 2	44 ± 3	12.6 ± 0.4	2.6 ± 0.1	141 ± 8	5.4 ± 0.3	40 ± 2
18th July	1.43 ± 0.01	16 ± 1	0.55 ± 0.02	0.51 ± 0.04	4.7 ± 0.2	0.03 ± 0.01	20.2 ± 0.6	12.9 ± 0.7	1.24 ± 0.06	2.6 ± 0.1	66 ± 3	0.74 ± 0.06	43 ± 2
22nd July	3.9 ± 0.2	16.9 ± 0.8	0.78 ± 0.01	1.15 ± 0.06	20.0 ± 0.5	5.1 ± 0.2	55 ± 2	25 ± 1	4.8 ± 0.2	2.01 ± 0.05	118 ± 4	1.87 ± 0.03	69 ± 3
26th July	6.94 ± 0.02	20 ± 1	< 0.36	0.80 ± 0.07	128 ± 3	10.1 ± 0.6	30 ± 1	16.9 ± 0.7	10.3 ± 0.3	3.6 ± 0.1	54 ± 2	10.3 ± 0.2	50 ± 3
30th July	6.7 ± 0.2	113 ± 3	2.0 ± 0.1	4.4 ± 0.4	46 ± 3	36 ± 2	168 ± 3	33 ± 1	13.9 ± 0.3	1.62 ± 0.08	118 ± 4	25 ± 2	320 ± 10
3rd August	10.8 ± 0.2	124 ± 2	2.2 ± 0.1	1.91 ± 0.01	68 ± 4	21 ± 1	115 ± 2	29 ± 2	23.1 ± 0.5	3.8 ± 0.2	197 ± 7	14.8 ± 0.8	187 ± 7
7th August	6.1 ± 0.3	21 ± 1	0.42 ± 0.03	0.82 ± 0.03	7.1 ± 0.2	2.86 ± 0.08	32 ±2	17 ± 1	6.7 ± 0.2	2.30 ± 0.07	61 ± 4	4.2 ± 0.2	41 ± 2
11th August	5.5 ± 0.3	26 ± 2	< 0.35	1.7 ± 0.1	9.2 ± 0.5	8.2 ± 0.3	74 ± 2	13.7 ± 0.8	13.6 ± 0.4	1.99 ± 0.06	340 ± 20	9.1 ± 0.6	24 ± 1
15th August	17 ± 1	36 ± 1	0.71 ± 0.03	0.82 ± 0.04	56 ± 1	33 ± 1	61 ± 2	81 ± 3	17.7 ± 0.3	2.59 ± 0.09	114 ± 4	14.6 ± 0.4	67 ± 3
19th August	5.0 ± 0.1	10.1 ± 0.7	< 0.37	0.44 ± 0.01	86 ± 2	3.8 ± 0.2	28.4 ± 0.7	40 ± 2	4.0 ± 0.1	1.08 ± 0.06	85 ± 3	4.4 ± 0.3	< 26.59
23th August	6.9 ± 0.2	18.7 ± 1	0.59 ± 0.03	1.68 ±0.06	14.3 ± 0.3	11.3 ± 0.6	32.3 ± 0.5	22 ± 1	8.9 ± 0.5	5.1 ± 0.2	320 ± 10	7.3 ± 0.5	46 ± 3
27th August	3.2 ± 0.2	56 ± 3	0.49 ± 0.05	2.0 ± 0.1	21.8 ± 0.8	6.0 ± 0.4	290 ± 10	52 ± 2	12.6 ± 0.5	1.09 ± 0.06	85 ± 2	0.90 ± 0.08	33 ± 2
31st August	1.76 ± 0.06	15.8 ± 0.3	< 0.36	0.63 ± 0.06	20.8 ± 0.7	0.52 ± 0.03	41 ± 2	21 ± 1	3.9 ± 0.1	2.8 ± 0.1	44 ± 1	1.8 ± 0.1	18.6 ± 0.7
4th September	12.7 ± 0.5	18.0 ± 0.3	1.5 ± 0.1	0.68 ± 0.06	15.2 ± 0.4	155 ± 2	36 ± 1	107 ± 7	10.3 ± 0.2	2.38 ± 0.08	< 8.2	3.10 ± 0.07	43 ± 1
8th September	8.9 ± 0.4	111 ± 4	< 0.55	4.4 ± 0.2	84 ± 2	25 ± 1	167 ± 9	91 ± 4	12.6 ± 0.4	5.6 ± 0.1	530 ± 20	18.4 ± 0.8	144 ± 9
12th September	6.35 ± 0.09	24 ± 1	0.57 ± 0.02	2.4 ± 0.1	48 ± 1	18.0 ± 0.7	58 ± 2	37 ± 2	26.4 ± 0.7	4.2 ± 0.3	58.0 ± 0.4	16.6 ± 0.5	73 ± 4
16th September	14.4 ± 0.9	210 ± 2	0.53 ± 0.04	10.8 ± 0.4	71 ± 2	32 ± 1	324 ± 4	67 ± 2	28.2 ± 0.7	2.25 ± 0.04	1,280 ± 40	41.4 ± 0.9	92 ± 4
20th September	6.3 ± 0.4	58 ± 4	1.59 ± 0.09	3.26 ± 0.09	18 ± 1	35 ± 1	120 ± 1	56 ± 2	13.1 ± 0.4	2.01 ± 0.09	260 ± 10	14.2 ± 0.7	104 ± 6
24th September	3.03 ± 0.01	103 ± 3	< 0.37	< 0.37	5.0 ± 0.2	55 ± 2	14.3 ± 0.8	12.2 ± 0.7	177 ± 3	7.7 ± 0.1	16.9 ± 0.8	0.96 ± 0.08	46 ± 3
28th September	4.6 ± 0.2	43 ± 2	< 0.33	2.37 ± 0.06	48 ± 1	147 ± 1	97 ± 3	35 ± 1	8.4 ± 0.3	3.28 ± 0.05	340 ± 10	11.6 ± 0.6	58 ± 3
2nd October	4.2 ± 0.1	107 ± 3	< 0.33	4.5 ± 0.3	134 ± 1	10.8 ± 0.5	185 ± 5	24 ± 1	15.9 ± 0.4	2.33 ± 0.08	320 ± 10	19.6 ± 0.6	37 ± 1
6th October	7.6 ± 0.7	26 ± 1	< 0.43	0.92 ± 0.08	14.9 ± 0.6	37 ± 3	34.4 ± 0.6	24 ± 1	11.3 ± 0.3	3.1 ± 0.2	139 ± 5	12.9 ± 0.9	55 ± 2
14th October	4.30 ± 0.04	81 ± 3	< 0.32	4.0 ± 0.1	39.8 ± 0.3	26.9 ± 0.5	253 ± 5	21.7 ± 0.6	11.4 ± 0.3	2.68 ± 0.06	289 ± 2	20.3 ± 0.6	48 ± 2
18th October	2.25 ± 0.01	21 ± 1	< 0.34	1.6 ± 0.1	47 ± 2	16.5 ± 0.6	42 ± 1	22 ± 1	5.27 ± 0.08	1.28 ± 0.04	98 ±4	2.8 ± 0.2	30 ± 1

Supplementary Table S5. Extraction percentages obtained for fraction I on the samples subjected to sequential extraction.

Sampling start date	Al	As	Ba	Ca	Cd	Co	Cr	Cu	Fe	K	Mg	Mn	Na	Ni	Pb	Sb	Ti	V	Zn
28th February	85	94	39	78	100	63	27	84	29	90	96	86	97	64	96	90	16	80	96
8th March	44	96	26	79	39	26	16	72	28	96	97	34	98	65	93	85	11	80	97
16th March	17	94	42	77	93	56	16	74	25	88	96	67	97	51	94	77	6	68	95
24th March	26	93	50	78	100	60	37	76	35	90	96	69	98	76	96	88	14	78	97
1st April	18	87	56	79	86	60	13	79	24	71	89	77	96	54	95	83	6	59	90
9th April	89	91	44	60	100	72	15	88	52	83	87	78	94	70	97	86	20	82	98
17th April	33	87	27	66	64	53	8	70	25	80	79	68	89	46	86	82	10	64	96
25th April	28	90	35	74	100	50	7	56	27	77	85	67	91	66	89	82	10	58	96
3rd May	20	84	31	70	100	60	8	68	24	77	87	13	94	77	84	66	5	54	94
11th May	52	88	29	69	100	55	7	60	33	78	74	65	84	28	93	84	14	56	98
23rd May	25	86	42	75	60	47	17	60	23	82	90	48	95	51	84	69	7	61	93
31st May	19	79	30	69	100	65	8	58	27	60	85	81	94	59	89	80	10	39	91
12nd June	12	64	27	88	69	50	7	68	26	39	86	68	93	40	75	66	7	27	96
20th June	39	87	34	70	100	57	9	74	36	80	88	68	94	54	95	85	15	68	93
2nd July	14	83	13	63	29	27	15	56	27	87	91	21	95	58	82	67	7	50	95
22nd July	8	75	19	54	65	35	4	67	22	81	81	51	87	46	72	62	9	46	93
3rd August	43	92	45	74	100	60	19	65	38	86	87	77	94	76	90	82	17	72	96
11th August	21	85	27	70	29	26	8	67	31	81	86	66	92	61	85	69	16	66	95
19th August	79	91	26	72	100	59	17	70	49	91	94	60	97	54	84	77	45	71	91
31st August	22	84	18	66	54	38	6	59	20	81	86	17	92	40	81	64	5	38	96
8th September	39	85	31	77	100	57	16	65	36	87	94	68	98	58	87	83	15	43	94
20th September	18	75	26	73	84	51	16	56	25	78	91	44	96	71	76	42	9	32	94
28th September	54	85	32	87	100	61	18	72	45	95	98	73	99	54	89	84	48	60	94
14th October	14	67	32	78	35	15	13	68	23	84	94	33	98	47	79	62	7	47	90

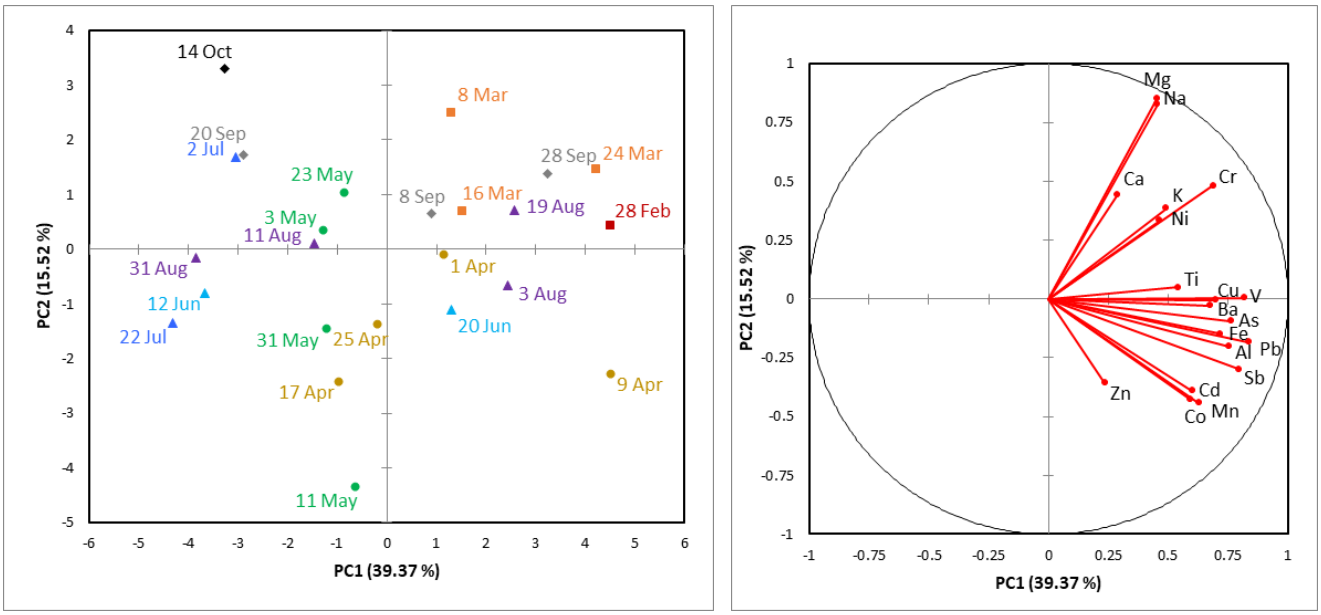

(**a**) (**b**)

Supplementary Figure S1. Principal Component Analysis performed on the results of the sequential extraction: (**a**) score and (**b**) loading plot.